Steel and Composite Structures, *Vol. 42, No. 4 (2022) 459-475*
https://doi.org/10.12989/scs.2022.42.4.459

Ultimate axial load of rectangular concrete-filled steel tubes using multiple ANN activation functions

Minas E. Lemonis[1], Angeliki G. Daramara[1], Alexandra G. Georgiadou[1], Vassilis G. Siorikis[1], Konstantinos Daniel Tsavdaridis[2] and Panagiotis G. Asteris[1*]

[1]*Computational Mechanics Laboratory, School of Pedagogical and Technological Education, 14121 Athens, Greece*
[2]*School of Civil Engineering, Faculty of Engineering and Physical Sciences, University of Leeds, Woodhouse Lane, West Yorkshire, Leeds LS2 9JT, U.K.*

(Received June 11, 2021 Revised December 20 2021, Accepted December 30, 2021)

Abstract. In this paper a model for the prediction of the ultimate axial compressive capacity of square and rectangular Concrete Filled Steel Tubes, based on an Artificial Neural Network modeling procedure is presented. The model is trained and tested using an experimental database, compiled for this reason from the literature that amounts to 1193 specimens, including long, thin-walled and high-strength ones. The proposed model was selected as the optimum from a plethora of alternatives, employing different activation functions in the context of Artificial Neural Network technique. The performance of the developed model was compared against existing methodologies from design codes and from proposals in the literature, employing several performance indices. It was found that the proposed model achieves remarkably improved predictions of the ultimate axial load.

Keywords: artificial neural network; CFST column; soft computing; ultimate axial load

1. Introduction

Steel is widely used for various structural components in the construction industry including civil, industrial, bridge, hydraulic etc. (Ali *et al*. 2016, Caprili and Salvatore 2015), due to its key properties that prove valuable in practice, such as high tensile and compressive strength, enhanced ductility, reliability as well as speed of construction (Zhao *et al*. 2015). However, the main disadvantage of structural steel is that it can be susceptible to corrosion and also the high cost of material (Young 2008). For example, a bare steel pipe under compression is susceptible to various instabilities, namely flexural buckling, local buckling etc. however, filling the pipe with concrete certain advantages are obtained. The corrosion resistance of the inner surface is enhanced, the buckling capacity as well as the local stability of the pipe walls against inward movement are increased and additionally, an elevated resistance to distortions, due to impact, is achieved (Khan *et al*. 2017). For the concrete core on the other hand, confinement is offered by the steel pipe, which also serves as formwork.

Steel tubes filled with concrete have shown many advantages in the literature and are widely used in many fields (Khanouki *et al*. 2016, Giakoumelis and Lam 2004). They are typically called concrete-filled steel tubes (CFSTs), and offer high strength and stiffness, large energy absorption capacity, high axial load capacity, attractive appearance, increased fire resistance, excellent ductility, and low strength degradation (Giakoumelis and Lam 2004). Having these characteristics, CFST components can be widely applied in many types of structures and loading conditions (Han and Yang 2001); for example as columns in high-rise buildings, in bridges (pylons, abutments, arch ribs, piers), and even in regions of high seismic risk (Tao *et al*. 2016, Song *et al*. 2017, Chang *et al*. 2012, Han *et al*. 2005, Baig *et al*. 2006). Notably, numerous bridges built in China have been using CFST-type components; for instance, 413 bridges with a span of no less than 50m were built in 2015 (Liu *et al*. 2019). In particular, CFST structures prove highly effective when subject to compression (Ren *et al*. 2019).

The maximum bearing capacity of CFST columns depends on the properties and behavior of its constituent materials. In addition, the behavior of columns depends on the geometric properties of the steel pipe, such as the width-to-thickness ratio and the confining effect of the steel pipe on the concrete core. The cross-sectional forms of the selected column CFST are usually symmetrical, either circular or square or rectangular (Han *et al*. 2014). The CFST columns with square and rectangular shapes are commonly used in construction, as they provide easier manufacturing process for the beam to column joints and achieve higher bending stiffness (Ren *et al*. 2019, Zhao *et al*. 2015). However, when compared to circular CFST columns, they do not offer the same confinement conditions and the potential for delamination of the concrete from the steel tube, under working loads, is increased (Krishan *et al*. 2016, Bradford *et al*. 2002, Goel and Tiwary 2018). It is well known that the bond-slip between the concrete core and the steel tube has a crucial effect on the mechanical

*Corresponding author, Associate Professor
E-mail: asteris@aspete.gr
E-mail: panagiotisasteris@gmail.com

http://www.techno-press.com/journals/scs&subpage=8 ISSN: 1229-9367 (Print), 1598-6233 (Online)

behavior, failure mode, and the working performance of the CFST members.

In the past decades, many studies of the bearing capacity and behavior of the CFST have been performed, focusing on their mechanical properties under axial compression. In Schneider (1998), a total of fourteen samples were used to evaluate the effect of wall thickness and the steel tube shape on the composite column ultimate strength, considering the parameters of the ratio of depth to tube wall thickness and the shape of the steel tube. The experimental results suggested that current design specifications are not sufficient for predicting the yield load for various structural shapes. Fam *et al*. (2004) carried out experimental work and analytical modeling of CFSTs subject to concentric axial compressive as well as lateral cyclic loading. Ten samples were tested; five short CFST column samples and five CFST beam-column samples. The results indicated that the bond and the end loading conditions had no significant influence on the flexural strength of beam-column members. Other studies also performed experimental tests focusing on the behavior of the CFST columns under the axial load (e.g., Ibanez *et al*. 2021, Yu *et al*. 2007, Han *et al*. 2012, Asteris *et al*. 2021c).

In addition, numerical simulations have been developed and widely applied in investigating the behavior of CFST columns under axial compression. For example, Dai *et al*. (2010) utilized Finite Element Modeling (FEM), to simulate the elliptical CFST columns under axial compression. Choi *et al*. (2009) described a numerical program for analyzing the behavior of the tubular CFST columns and predicting different modes of lateral interactions between the concrete and the steel tube under axial compression. It is worth noting that in such numerical simulations, it is laborious to take into account all material properties and interactions, in order for the models to be able to predict the behavior of the CFST columns, under various loading conditions and with a reasonable precision (Sarir *et al*. 2019b). From previous studies, many well-known national standards and recommendations proposed various practical design formulas in order to characterize the behavior of the CFST columns, namely Chinese code DBJ 13-51-2010 (2010), Australian code AS5100 (2004), American code AISC 360 (2016), Japanese code AIJ (1997), and European code EN1994 (2004). Moreover, other simplified calculation formulas have also been proposed, for instance, Yu *et al*. (2013) proposed a unified formula to calculate the axial load-bearing capacity of the circular or polygonal CFST columns. However, most simplified methodologies suffer from limited application scope and/or accuracy, preventing them from widespread use. Therefore, the development of robust and accurate methods for multiple applications are required to be able to calculate with confidence the final load-bearing capacity of the CFST columns.

Artificial Intelligence (AI) and machine learning have been developed and applied in many different fields with high precision and effectiveness (Ahmadi *et al*. 2017, Psyllaki *et al.* 2018, Kechagias *et al.* 2018, Huang *et al.* 2019, Apostolopoulou *et al.* 2019, 2020, Armaghani *et al.* 2020, Armaghani and Asteris 2021, Asteris *et al*. 2021a, 2021b, Zeng *et al.* 2021, Zhang *et al.* 2021). Out of these,

Table 1 Field of application of examined design codes regarding CFST axial compressive strength

Code	Limits
EN1994 (2004)	$235 \leq f_y \leq 460$ $25 \leq f_c' \leq 50$ $H/t \leq 52\sqrt{(235/f_y)}$
AISC 360 (2016)	$f_y \leq 525$ $21 \leq f_c \leq 69$ $H/t \leq 5\sqrt{(E_s/f_y)}$
AIJ (1997)	$235 \leq f_y \leq 355$ $18 \leq f_c' \leq 60$ $H/t \leq 1102.5/\sqrt{\min\{f_y; 0.7f_u\}}$
AS5100 (2004)	$f_y \leq 350$ $25 \leq f_c' \leq 65$ $H/t\sqrt{(f_y/250)} \leq a$ where a depends on tube manufacturing

Artificial Neural Network (ANN), which uses existing experimental data to train neural networks in order to study the behavior of the materials and structures under various testing conditions, has become the most commonly used machine learning algorithm (Jegadesh and Jayalekshmi 2015, 2015b). Many studies related to ANN on the behavior of steel-concrete pipe columns, subject to different types of loads have been conducted, such as the estimation of fire resistance of tubular CFST columns (Al-Khaleefi *et al*. 2002); study of biaxial bending behavior of steel-concrete composite beam-columns (Behnam and Esfahani 2018) and ultrasonic testing CFST (Xiao 2012). Du *et al.* (2017) utilized ANN to estimate the axial bearing capacity of rectangular CFST columns, considering various input parameters, namely sectional width, length and thickness, steel and concrete strength. In such a study, a total of 305 experimental samples were collected, and the results showed that the predicted values are more accurate compared to ACI-318 (2014) and EN1994 (2004). Focusing on the same problem, a growing number of works employs soft computing techniques, including Duong *et al.* (2020), Ly *et al*. (2021), Asteris *et al.* (2021a), Ho and Le (2021). An in-depth state-of-the-art review on the behavior of CFST columns has been recently published by Sarir *et al*. (2019a), where two ANN-based hybrid metaheuristic models were presented, optimized by whale optimization algorithm (WOA) and particle swarm optimization (PSO). Validation and comparison results confirmed the effective role of the WOA in optimization of the proposed hybrid model (ANN-WOA) to predict the bearing capacity of CFST columns.

In the present study, available experimental results for the ultimate axial loads of rectangular concrete-filled steel tubes (CFST) are selected and incorporated within a database of tested specimens.

2. Research significance

Structural engineers spend significant amount of time in preliminary design stage and optimization. Artificial Neural Network (ANN) has been emerging quickly in the research field, but more practical examples are required to increase

Table 2 Expressions in the literature for the CFST axial compressive strength

Source	Formulas	Source	Formulas
Sakino *et al.* (2004)	$N^{Sakino2004} = A_s\sigma_{scr} + A_c\gamma_U f_c'$ – $\sigma_{scr} = Sf_y \le f_y$ – $\frac{1}{S} = 0.698 + 0.128\left(\frac{H}{t}\right)^2 \frac{f_y}{E_s}\frac{4.00}{6.97}$ – $\gamma_U = 1.67D_c^{-0.112}$ – D_c = diameter of circle, with same area	Wang *et al.* (2017)	$N^{Wang2017} = \eta_\alpha f_y A_s + \eta_c f_c' A_c$ – $\eta_\alpha = 0.91 + \left(7310f_y - \left(128 + 2.26f_y\right)\left(\frac{W}{t}\right)^2\right)10^{-8}$ – $\eta_c = 0.98 + 29.5f_y^{-0.48}k_s^{0.2}\left(\frac{tf_y}{Wf_c'}\right)^{1.3}$ – $k_s = \frac{1}{3}\left(\frac{B-2t}{H-2t}\right)^2$ – $W = \sqrt{H^2 + B^2}$
Han *et al.* (2005)	$N^{Han2005} = f_{scy}(A_s + A_c)$ – $f_{scy} = f_c'(1.18 + 0.85\xi)$ – $\xi = A_s f_y / A_c f_c'$	Du *et al.* (2016)	$N^{Du2016} = f_y A_s + (1+k)f_c' A_c$ – $k = 0.5668 - 0.0039\frac{H}{t}\sqrt{\frac{f_y}{235}}$

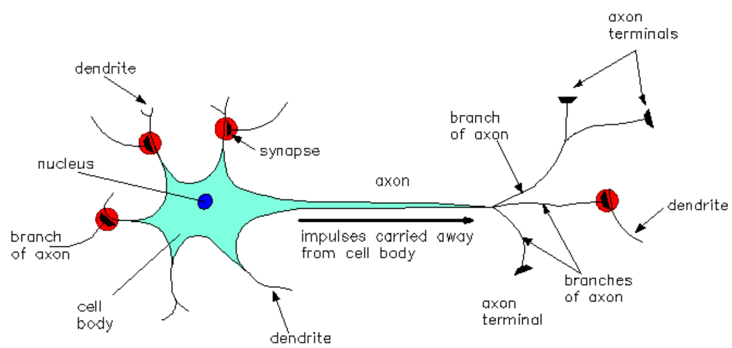

Fig. 1 Schematic representation of the biological neuron structure (Asteris et al. 2019)

confidence is using it while ANN has becoming popular in the ACE sector. This study evaluates the feasibility of ANN in designing CFST columns used in the building construction sector to help increase the efficiency in design stages. ANN has been selected as it has the ability to learn and model non-linear and complex relationship which fits to most structural design problems. The evaluation of the feasibility to utilize ANN is important for the future of structural design as Artificial Intelligence (AI) models can optimize and predict, as well as increase the efficiency at preliminary design stage.

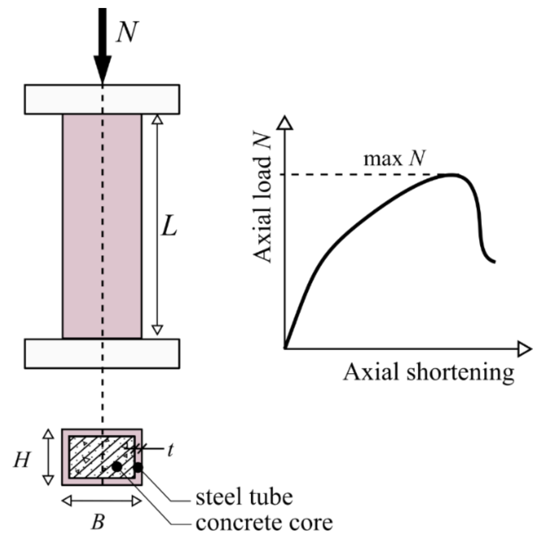

Fig. 2 Rectangular CFST under uniaxial compressive load

3. Brief literature review on available proposals

Many steel and composite codes cover the design of CFST columns subject to axial compression. These include the European code EN1994 (2004), the American codes AISC 360 (2016) and ACI-318 (2014), the Japanese code AIJ (1997), the Australian code AS5100 (2004), and the Chinese code DBJ 13-51-2010 (2010). All codes limit their field of application, typically in regard to steel strength f_y, concrete strength f_c' and steel section slenderness. Table 1 presents these limits for EN1994 (2004), AISC-360 (2016), AIJ (1997) and AS5100 (2004), that will be utilized in this work for comparison against the proposed ANN methodology, later in the text. It can be seen that a significant range of high strength steels and concretes is not covered by the codes. AISC-360 (2016) is the most

Table 3 Data from experiments published in literature

Nr.	Reference	Number of Samples			Axial Load
		Tested	Inverted	Total	(kN)
1	Zhang 1984	50		50	660,00-2800,00
2	Lu *et al.* 1999	6		6	2061,00-4872,00
3	Guo 2006	6		6	347,00-1785,00
4	Liu and Gho 2005	14	6	20	1566,00-3996,00
5	Liu *et al.* 2003	6	6	12	1490,00-4210,00
6	Liu Dalin 2005	10	2	12	1657,00-2828,00
7	Ye Zaili 2001	45	21	66	1150,00-2700,00
8	Guo *et al.* 2006	8		8	635,00-1785,00
9	Wei and Han 2000	20		20	882,00-2058,00
10	Zhang and Zhou 2000	36		36	588,00-1323,00
11	Tomii and Sakino 1979	8		8	497,40-667,00
12	Inai and Sakino 1996	46		46	1153,00-7780,00
13	Nakahara and Sakino 1998	4		4	3899,00-6645,00
14	Lu and Kennedy 1992	4	2	6	1906,00-4208,00
15	Yamamoto 2000	16		16	411,00-6494,00
16	Lam and Williams 2004	15		15	680,00-2000,00
17	Han and Yao 2004	6		6	2284,00-2594,00
18	Matsui *et al.* 1995	5		5	1143,00-1598,00
19	Wei and Han 2000	8		8	754,20-2082,50
20	Furlong 1967	10		10	488,00-1601,36
21	Grauers 1993	14		14	1440,00-2680,00
22	Schnider 1998	11	9	20	819,00-2069,00
23	Chung *et al.* 2001	5		5	1144,00-1598,00
24	Han 2002	4	4	8	740,00-880,00
25	Ghannam 2004	14	12	26	491,00-1248,00
26	Han and Yao 2004	5		5	1986,00-2280,00
27	Guo *et al.* 2005	10	4	14	1558,00-2636,00
28	Luo 1986	28		28	600,00-1740,00
29	Liu and Gho 2005	12	12	24	1725,00-2291,00
30	Liu *et al.* 2003	15	15	30	1425,00-2970,00
31	Liu 2005	12	12	24	1735,00-2124,00
32	Ye 2001	23	23	46	1068,00-2700,00
33	Knowles and Park 1969	6		6	355,86-511,55
34	Lin 1988	12	6	18	558,00-1268,00
35	Shakir-Khalil and Mouli 1990	14	14	28	850,00-1370,00
36	Matsui and Tsuda 1996	5		5	1143,46-1597,50
37	Han and Yao 2003a	19	15	34	552,00-1140,00
38	Han and Yang 2003	4	4	8	490,00-825,00
39	Han and Yao 2003b	6		6	640,00-816,00
40	Ghannam *et al.* 2004	24	12	36	240,00-1248,00
41	Han and Yao 2004	11		11	1986,00-2594,00
42	Sakino *et al.* 2004	46		46	1153,00-7780,00
43	Yu *et al.* 2008	10		10	466,00-1220,00
44	Aslani *et al.* 2015	12		12	1367,00-3882,00
45	Du *et al.* 2016a	6	5	11	3090,00-3575,00
46	Du *et al.* 2016b	8	8	16	1960,00-3150,00
47	Dundu 2016	27		27	105,40-1516,26
48	Khan *et al.* 2017a	39		39	286,00-6329,00
49	Khan *et al.* 2017b	16		16	1636,00-7506,00
50	Mursi and Uy 2004	4		4	1835,00-3950,00
51	Vrcelj and Uy 2002	8	5	13	269,00-684,00
52	Xiong *et al.* 2017	5		5	6536,00-7276,00
53	Zhu *et al.* 2017	6		6	2730,00-3980,00
54	Lue *et al.* 2007	22	22	44	1281,30-2196,40
55	Liew *et al.* 2016	5		5	6536,00-7276,00
56	Chen *et al.* 2018	9		9	987,00-2051,00
57	Ibanez *et al.* 2018	6	2	8	824,50-1882,50
58	Zhu and Chan 2018	7		7	3452,00-6298,00

Table 3 Data from experiments published in literature

Nr.	Reference	Number of Samples			Axial Load
		Tested	Inverted	Total	(kN)
59	Uy 1998	5		5	950,00-2519,00
60	Uy 2000	8		8	1114,00-4581,00
61	Tao *et al.* 2009	4		4	1993,00-3190,00
62	Tao et al. 2008	6		6	2140,00-4080,00
63	Cederwall *et al.* 1990	14		14	1380,00-2680,00
64	Chen and Jin 2010	6	5	11	1980,00-2360,00
65	Han *et al.* 2005	24		24	318,00-3400,00
66	Lu *et al.* 2021	4		4	7246,00-9057,00
67	Yan *et al.* 2020	6	6	12	1000,00-1314,00
68	Ibanez *et al.* 2021	8	4	12	824,50-1882,50
69	Hossain and Chu 2019	13	3	16	176,00-1535,00
70	Huang *et al.* 2020	10	10	20	3203,80-4250,10
71	Zhou *et al.* 2020	4		4	5322,00-7945,00
72	Islam *et al.* 2021	13		13	770,00-1384,00
73	Nguyen *et al.* 2021	6		6	2216,00-3154,00
	Total	944	249	1193	105,40-9057,00

Table 4 The input and output parameters used in the development of BPNNs

Variable	Symbol	Units	Category	Data in NN Models			
				Min	Average	Max	STD
Width of Tubes Section	B	mm	Input	50.00	142.48	400.00	51.50
Height of Tubes Section	H	mm	Input	50.00	142.48	400.00	51.50
Thickness of Tubes	t	mm	Input	0.70	4.28	10.30	1.68
Effective Length of Column	Le	mm	Input	60.00	906.03	3600.00	791.60
Steel Yield Strength	fy	MPa	Input	176.30	406.02	1030.60	172.28
Concrete Compressive Strength	f'c	MPa	Input	8.50	51.95	150.97	28.87
Axial Load	N	KN	Output	105.40	2003.27	9057.00	1502.36

Table 5 Correlation matrix of the input and output variables

Variables		Input						Output
		B	H	t	Le	fy	f'c	N
Input	B	1.00						
	H	0.75	1.00					
	t	0.10	0.10	1.00				
	Le	0.01	0.01	-0.08	1.00			
	fy	-0.02	-0.02	0.38	0.11	1.00		
	fc'	-0.06	-0.06	0.19	0.03	0.27	1.00	
Output	N	0.65	0.65	0.50	-0.10	0.51	0.32	1.00

inclusive one, particularly regarding steel.

All examined codes provide procedures for validating the squash load of CFST using a combination of the plastic strengths of the steel and concrete parts. For slender steel sections however, the ultimate compressive capacity is restricted by the local buckling phenomena of the tube walls. On the other hand, for long columns, the ultimate load is probably determined by member buckling. axial compressive load. The selected codes provide methodologies for the characterization of local or global buckling phenomena. Taking into account that the specimens in our experimental database, that will be presented later in the text, contain both long tubes and thin-walled ones, this remark is considered crucial for a fair comparison between the design codes. Safety factors are not included in the presented formulas. Appendix presents the relevant formulas available in the four selected design codes for the calculation of the CFST capacity, under.

A significant number of proposals is also available in the literature for the estimation of the axial ultimate load of square and rectangular CFSTs. Among others, Sakino *et al.* (2004) proposed a strength reduction factor, for square shaped tubes, accounting for local instabilities. Han *et al.* (2005), provided an expression for the squash load of square and circular CFSTs. Wang *et al.* (2017) proposed a simplified model for the prediction of the ultimate axial load of circular and rectangular CFST columns, accounting for concrete confinement and tube slenderness. Also, for high strength steel, Du *et al*. (2016) calibrated an expression for the ultimate load of CFSTs. Table 2 summarizes these expressions available in the literature, in the case of rectangular tubes, that is the scope of this work.

4. Materials and methods

4.1 Brief review on artificial neural networks

Artificial neural networks (ANNs) are based on the concept of the biological neural network of the human brain. The basic building block of ANNs is the artificial neuron, which is a mathematical model aiming to mimic the behavior of the biological neuron (Fig. 1). Information is passed into the artificial neuron as input and is processed with a mathematical function leading to an output that determines the behavior of the neuron (similar to fire-or-not situation for the biological neuron). Before the information enters the neuron, it is weighted in order to approximate the random nature of the biological neuron. A group of such neurons consists of an ANN, in a manner similar to biological neural networks. In order to set up an ANN, one needs to define: (i) the architecture of the ANN; (ii) the training algorithm, which will be used for the ANN's learning phase; and (iii) the mathematical functions describing the mathematical model.

The architecture or topology of the ANN describes the manner in which the artificial neurons are organized in the group and how information flows within the network. For example, if the neurons are organized in more than one layer, then the network is called a multilayer ANN. The training phase can be considered as a function minimization problem, in which the optimum values of weights need to be determined by minimizing an error function. Depending on the optimization algorithms used for this purpose, different types of ANNs exist.

The gradient descent (GD) method is employed mainly in the back-propagation (BP) stage of the training process of the ANN model (Rumelhart *et al*. 1986). The main working principle of the GD is to adjust the weights of the ANN model iteratively while minimizing the error between the actual output and target (Du and Swamy 2013). However, using GD may results to convergence problems (Gupta *et al*. 2013) (i.e., time-consuming training process). Many more training algorithms have been proposed to enhance the effectiveness of ANN training, one of them is the Levenberg-Marquardt (LM) method (Marquardt 1963), which has been commonly used in various studies of different fields (Raghuwanshi *et al*. 2006, Aqil *et al*. 2007, de Vos and Rientjes 2008, Taormina *et al*. 2012). The speed of convergence when using the LM technique has been improved due to the method that was developed by combining the GD and Gauss-Newton (GN) algorithms (Marquardt 1963). More recently, a number of training algorithms that use the second derivative have been proposed in the literature. These are the One-Step Secant (OSS) (Battiti 1992), the Gradient Descent with Adaptive Learning Rate (GDA) (Kayacan and Khanesar 2015), the Scaled Conjugate Gradient (SCG) (Møller 1993), and the Conjugate Gradient Backpropagation with Powell-Beale Restarts (CGB) (Powell 1977). However, second-order learning techniques require to be used in a batch mode due to the sensitivity of the numerical computation of second-order gradients (Akbar *et al*. 2011, Du and Swamy 2013). In addition, learning algorithms based on the first and second-order derivative may not have the required convergence ability if the starting point is located outside of the search domain (Brownlee 2016). The foresaid learning algorithms contributed to the progress in training ANN methods, for better performance of the prediction models.

4.2 Performance Indices

Three different statistical parameters were employed to evaluate the performance of the derived computational model as well as the available in the literature formulae, including the root mean square error (RMSE), the mean absolute percentage error (MAPE), and the Pearson Correlation Coefficient R^2. The lower RMSE and MAPE values represent the more accurate prediction results. The higher R^2 values represent the greater fit between the analytical and predicted values. The aforementioned statistical parameters have been calculated by the following expressions (Alavi and Gandomi 2012):

$$RMSE = \sqrt{\frac{1}{n}\sum_{i=1}^{n}(x_i - y_i)^2} \tag{1}$$

$$MAPE = \frac{1}{n}\sum_{i=1}^{n}\left|\frac{x_i - y_i}{x_i}\right| \tag{2}$$

$$R^2 = 1 - \left(\frac{\sum_{i=1}^{n}(x_i - y_i)^2}{\sum_{i=1}^{n}(x_i - \bar{x})^2}\right) \tag{3}$$

where n denotes the total number of datasets, and x_i and y_i represent the predicted and target values, respectively.

The reliability and accuracy of the developed neural networks were evaluated using Pearson's correlation coefficient R and the root mean square error (RMSE). RMSE presents information on the short-term efficiency which is a benchmark of the difference of predicted values in relation to the experimental values. The lower the RMSE, the more accurate is the evaluation. The Pearson's correlation coefficient R measures the variance that is interpreted by the model, which is the reduction of variance when using the model. R values range from 0 to 1, however the model has healthy predictive ability when it is near to 1 and it is not predicting when near to 0. These performance metrics are a good measure of the overall predictive accuracy.

Furthermore, the following new engineering index, called a20-index, has been proposed for the reliability assessment of the developed ANN models (Asteris *et al*. 2019, Asteris and Mokos 2020, Asteris *et al*. 2021d):

$$a_{20-index} = \frac{m20}{M} \tag{4}$$

where M is the number of dataset sample and m20 is the number of samples with value of rate Experimental value/Predicted value between 0.80 and 1.20. Note that for a perfect predictive model, the values of a20-index values are

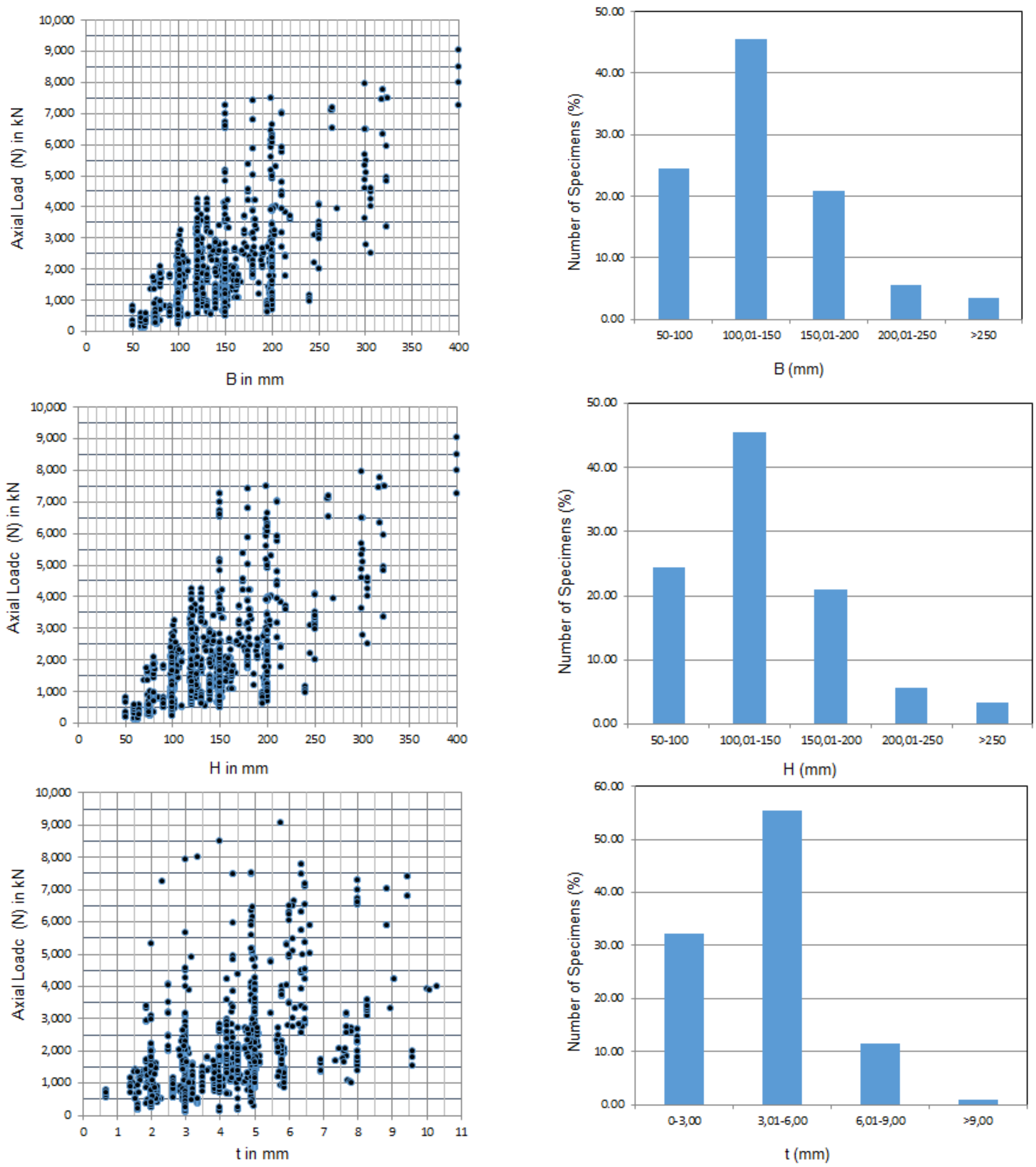

Fig. 3 Histograms of the parameters: Length of Tubes Section (B); Height of Tubes Section (H) and Thickness of Tubes Section (t)

expected to be unity. The proposed a20-index has the advantage that their value has a physical engineering meaning. It declares the amount of the samples that satisfies predicted values with a margin ±20% compared to experimental values.

4.3 Data used and selection of variables

It should be noted that the term "sufficient amount of data" does not necessarily imply a high amount of data, but rather datasets that cover a wide range of combinations of input parameter values, thus assisting in the model capability to simulate the problem. The demand for a reliable database is particularly crucial in the case of experimental databases, which are databases compiled using experimental results. In this case, significant deviations between experimental values are frequently noticed, not only between experiments conducted by different research teams and laboratories, but even between datasets derived from experiments conducted on specimens of the same synthesis, produced by the same technicians,

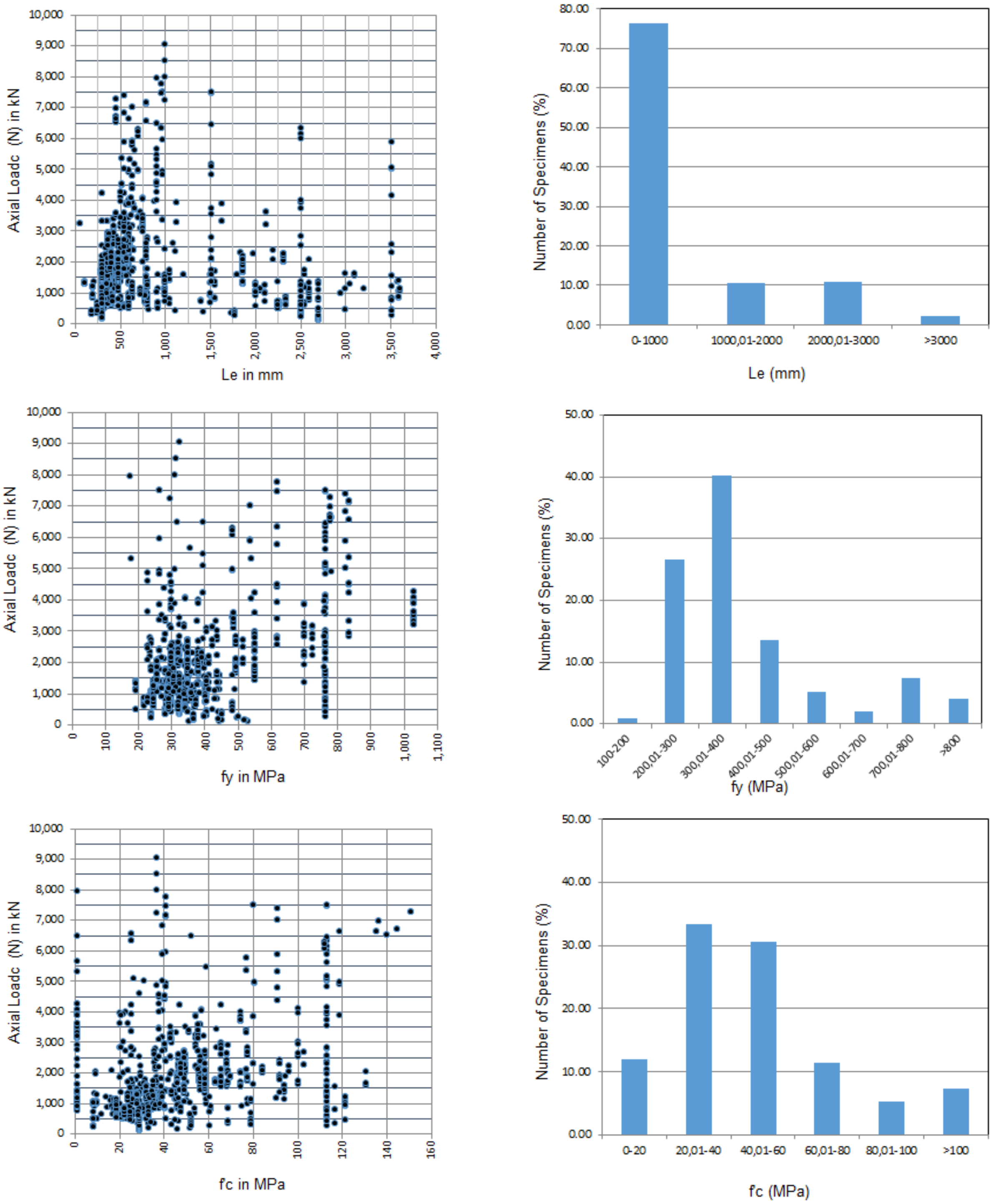

Fig. 4 Histograms of the parameters: Effectivr Length of Steel Tube Column (Le); Steel Yield Strength (fy) and Concrete Compressive Strength (fc')

cured under the same conditions and tested implementing the same standards and the same testing instruments.

In light of the above discussion, an experimental database comprising 1193 datasets was compiled from research papers reported in the literature dealing with the behavior of rectangular concrete-filled steel tubes under axial load without any eccentricity (Fig. 2).

Table 3 presents in detail the number of samples and the range of ultimate axial load for each one of the 73 experimental works used for the compilation of the database which will be used for the development and training of the soft computing model in the context of the artificial neural network technique. Each dataset comprises of six input parameters (Width of Tube Section (B), Height of Tube

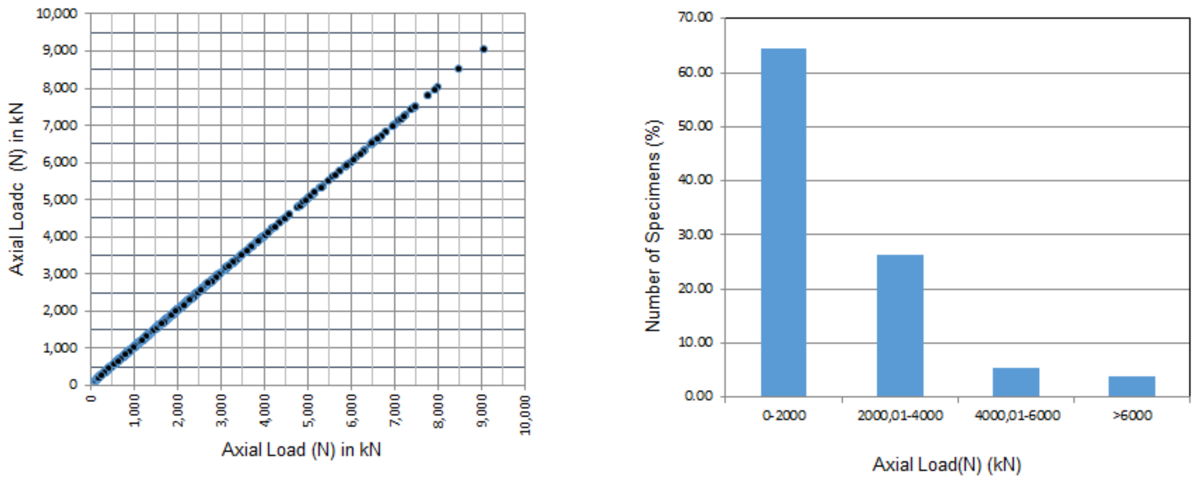

Fig. 5 Histograms of the parameters of the ultimate axial load (N)

Section (H), Thickness of Tube (t), Effective Length of Column (Le), Steel Yield Strength (fy) and Concrete Compressive Strength (f'c)) and the ultimate axial load (N) as the output parameter. Table 4 shows the minimum average and maximum values, as well as the standard deviation of the input and output parameters respectively, while Table 5 presents the correlation matrix of the input and output parameters. The histograms for each of the input and output parameters are presented in Figs. 3 to 5.

4.4 Sensitivity analysis

In general, sensitivity analysis (SA) of a numerical model is a technique used to determine if the output of the model is affected by changes in the input parameters. This provides feedback regarding which input parameters are the most significant, and thus, by removing the insignificant ones, the input space will be reduced and subsequently the complexity of the model, as well as the time required for its training, will be also reduced. In order to identify the effects of model inputs on the outputs, the SA can be conducted on the database. Sometimes, the results of SA help researchers/designers to remove one or more input parameters from the database to obtain better analyses with a higher level of performance prediction. To perform the SA, the cosine amplitude method (CAM), is employed, which has been used by many researchers (Armaghani and Asteris 2021, Armaghani *et al.* 2015, 2020, Momeni *et al.* 2015, Asteris *et al*. 2021). In CAM, data pairs may be used to construct a data array, X, as follows:

$$X = \{x_1, x_2, x_3, \ldots, x_i, \ldots, x_n\} \tag{5}$$

Variable x_i in array, X, is a length vector of m as:

$$x_i = \{x_{i1}, x_{i2}, x_{i3}, \ldots, x_{im}\} \tag{6}$$

The relationship between R_{ij} (strength of the relation) and datasets of X_i and X_j is presented by the following equation:

$$R_{ij} = \frac{\sum_{k=1}^{m} x_{ik} x_{jk}}{\sqrt{\sum_{k=1}^{m} x^2{}_{ik} \sum_{k=1}^{m} x^2{}_{ik}}} \tag{7}$$

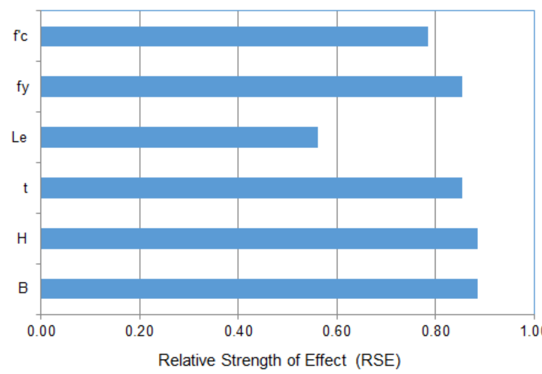

Fig. 6 Sensitivity analysis of Axial Load Capacity of Rectangular Concrete-filled Steel Tube Columns

The R_{ij} values between the Axial Load Capacity of Rectangular Concrete-filled Steel Tube Columns and the input parameters are shown in Fig. 6. This analysis reveals that, the width and the height of the steel tube cross section have the greatest influence on axial load capacity values, with strength values of 0.8841, followed by steel yield strength, f_y (0.8550), thickness of tube walls, t (0.8540), concrete compressive strength, f_c' (0.7852). The parameter with the lowest influence on axial load capacity seems to be the effective column length, L_e (0.5614).

5. Results and discussion

5.1. Development of ANN models

Based on the above, different architecture ANNs were developed and trained. More specifically, during the development and training of the ANN models the following steps (which are summarized in Table 6 was followed:

• The 1193 datasets in the database, used for the training and development of the ANN models, were divided into three separate sets. Specifically, 796 of 1193 (66.72%) datasets were

Table 6 Training parameters of ANN models

Parameter	Value	Matlab function
Training Algorithm	Levenberg-Marquardt Algorithm	trainlm
Normalization	Minmax in the range [0.10 – 0.90] and [-1.00-1.00] Zscore	Mapminmax zscore
Number of Hidden Layers	1	
Number of Neurons per Hidden Layer	1 to 30 by step 1	
Control random number generation	10 different random generation	rand(seed, generator), where generator range from 1 to 10 by step 1
Training Goal	0	
Epochs	200	
Cost Function	Mean Square Error (MSE)	mse
	Sum Square Error (SSE)	sse
Transfer Functions	Hyperbolic Tangent Sigmoid transfer function (HTS)	tansig
	Log-sigmoid transfer function (LS)	logsig
	Linear transfer function (Li)	purelin
	Positive linear transfer function (PLi)	poslin
	Symmetric saturating linear transfer function (SSL)	satlins
	Soft max transfer function (SM)	softmax
	Competitive transfer function (Co)	compet
	Triangular basis transfer function (TB)	tribas
	Radial basis transfer function (RB)	radbas
	Normalized radial basis transfer function (NRB)	radbasn

Table 7 Best twenty optimum architectures of ANN models based on Testing datasets RMSE index

Ranking	Normalization Technique	Cost Function	Transfer Function		Architecture	Epochs	Datasets	
							Testing	
			Input Layer	Output Layer			R	RMSE
1	Zscore	MSE	satlins	purelin	6-30-1	24	0.9923	186.12
2	Minmax [-1.00, 1.00]	MSE	logsig	tansig	6-24-1	16	0.9923	186.66
3	Minmax [-1.00, 1.00]	MSE	tansig	tansig	6-16-1	52	0.9923	186.76
4	Zscore	MSE	tansig	purelin	6-27-1	10	0.9922	188.31
5	Minmax [-1.00, 1.00]	SSE	satlins	satlins	6-25-1	52	0.9920	190.08
6	Minmax [-1.00, 1.00]	SSE	logsig	tansig	6-24-1	16	0.9919	190.59
7	Minmax [0.10, 0.90]	SSE	satlins	logsig	6-20-1	24	0.9919	190.84
8	Minmax [-1.00, 1.00]	MSE	tansig	tansig	6-24-1	52	0.9919	191.21
9	Minmax [-1.00, 1.00]	SSE	tansig	tansig	6-24-1	52	0.9919	191.35
10	Zscore	SSE	softmax	purelin	6-20-1	10	0.9919	191.62
11	Minmax [0.10, 0.90]	SSE	radbasn	logsig	6-29-1	24	0.9919	191.69
12	Zscore	MSE	logsig	purelin	6-28-1	10	0.9918	192.23
13	Minmax [-1.00, 1.00]	MSE	radbasn	tansig	6-23-1	16	0.9918	192.36
14	Zscore	MSE	tansig	purelin	6-23-1	26	0.9918	192.55
15	Minmax [0.10, 0.90]	SSE	radbas	logsig	6-19-1	56	0.9918	192.58
16	Minmax [0.10, 0.90]	MSE	radbasn	logsig	6-21-1	56	0.9917	193.70
17	Minmax [-1.00, 1.00]	SSE	logsig	purelin	6-16-1	12	0.9917	193.85
18	Minmax [-1.00, 1.00]	MSE	tribas	satlins	6-26-1	12	0.9916	193.86
19	Minmax [0.10, 0.90]	MSE	radbasn	purelin	6-24-1	24	0.9917	193.86
20	Minmax [0.10, 0.90]	SSE	radbasn	radbas	6-29-1	56	0.9917	194.01

designated as Training datasets, 199 (16.68%) as Validation datasets, while 198 (16.60%) datasets were used as Testing datasets.

• During the training of the ANNs, the above datasets were used with and without normalization. When normalization of the data was conducted, the minmax normalization technique in the range [0.10, 0.90] and [-1.00, 100) as well as the Zscore were implemented.

• The Levenberg–Marquardt algorithm (Lourakis 2005) was used for the training of the ANNs.

• 10 different initial values of weights and biases were applied for each architecture (Table 6).

• ANNs with only one hidden layer were developed and trained.

• The Number of Neurons per Hidden Layer ranged from 1 to 30, by an increment step of 1.

• Two functions, the Mean Square Error (MSE) and Sum Square Error (SSE) functions were used as cost functions, during the training and validation process.

• 10 functions, as presented in Table, were used as transfer or activation functions

The above steps resulted in the development of 240.000

Table 8 Summary of prediction capability of the optimum BPNN 6-30-1 model against existing methodologies

	Model	Datasets	Performance Indices				
			a20-index	R	RMSE	MAPE	VAF
1	BPNN 6-30-1	Training	0.9209	0.9888	**227.37**	0.1100	97.78
		Test	0.9246	0.9923	**186.12**	0.0888	98.47
2	Wang *et al.* (2017)	Test	0.7638	0.9704	**382.82**	0.1475	93.51
3	EN1994 (2004)	Test	0.7588	0.9697	**400.86**	0.1731	93.72
4	AIJ (1997)	Test	0.6533	0.9669	**421.48**	0.2011	93.49
5	Sakino *et al.* (2004)	Test	0.6884	0.9639	**421.53**	0.1840	92.88
6	AS5100 (2004)	Test	0.7688	0.9628	**435.91**	0.1929	92.14
7	AISC360 (2016)	Test	0.5779	0.9691	**479.52**	0.2426	93.85
8	Han *et al.* (2005)	Test	0.7136	0.9588	**615.84**	0.1945	86.25
9	Du *et al.* (2016)	Test	0.6432	0.9565	**640.80**	0.1984	85.35

different ANNs. It is worth noting that only the use of 10 different transfer function results in 100 different ANNs, for each architecture with the same number of neurons, as a result of 100 (=10^2) different dual combinations of the 10 transfer functions investigated.

The above developed 240.000 ANNs were ranked based on the value of the RMSE performance index, for the case of Testing Datasets, and the top 20 architectures are presented in Table 7. Among them, the optimum ANN model, based on the value of RMSE of Testing Datasets, is the BPNN 6-30-1 model that corresponds to a NN structure with 30 neurons, and use of zscore normalization technique, while the transfer functions are the Symmetric saturating linear transfer function (SSL) (satlins) for the hidden layer and the Linear transfer function (Li) (purelin) for the output layer.

5.2. Evaluation

Table 8 summarizes the prediction capability of the optimum BPNN 6-30-1 both for training and testing datasets for the five used performance indices (a20-index, R, RMSE, MAPE and VAF). A remarkably high a20-index, over 0.92, indicates that 92% of the specimens were predicted with a margin of error 20%. In the same table, the performance indices of existing methodologies in the design codes and the literature, that were described in a previous section, are also presented, for the Testing datasets. The methodologies are sorted according to their RMSE index. It can be observed that the developed ANN model outperforms existing methodologies for all examined performance indices. Taking into account the Testing Dataset for the comparison, the BPNN 6-30-1 achieves more than 50% reduction of RMSE, compared to the best existing methodology in this regard, which is the proposed by Wang *et al.* (2017). Also, the proposed ANN model records a 20% increase of the a20-index, compared to the Australian AS5100 (2004) code, which performs better among existing methodologies in this index.

Among the design codes, the best RMSE index is achieved by the European EN1994 (2004) code, closely followed by the Japanese AIJ (1997) and Australian AS5100 (2004) ones. In terms of a20-index the AS5100 (2004) and EN1994 (2004) perform quite similar, with a small improvement maintained by the former. American AISC 360 (2016) code achieves the best VAF index among the examined codes however, the remaining indices are worst. Comparing between the methodologies from the literature, the model form Wang *et al.* (2017) achieves the best indices overall. The model from Sakino *et al.* (2004) follows in terms of RMSE index while the model from Han *et al.* (2005) achieves the second best a20-index. The models from Han *et al.* (2005) and Du et al. (2016), which feature simpler formulations, present quite lower RMSE indices.

6. Conclusions

In this paper, a new model for the prediction of the ultimate load of square and rectangular CFSTs under axial compression was presented. The model is based on the ANN technique and employs a number of 30 neurons in a single hidden layer. Its development employed a number of different activation functions and normalization techniques and it was selected as the optimum from 240000 alternative configurations tested and compared with several performance indices. The following points are the main conclusions from the development procedure:

• The proposed model predicts the ultimate axial load in a quite satisfactory manner offering 20% error margin for 92% of the specimens. Against existing methodologies from the literature and design codes the improvement proves quite significant.

• For the optimum ANN model, it was found that the zscore transfer function provided the better prediction capability compared to liner scaling in a predetermined value ranges that is typically employed. Regarding transfer activation functions the Symmetric Saturating Linear transfer function (SSL) proved more effective for the hidden layer and the Linear transfer function (Li) for the output layer.

• According to results from sensitivity analysis, among the several input variables, the most influencing ones proved the tube dimensions followed by the steel yield limit.

The effective range of input parameters used for the development of the proposed ANN model also defines its valid field of application. Regarding member slenderness, ratios of L/min{B;H} up to 24 have been effectively used, whereas for section slenderness, ratios of max{B;H}/t up to 110. Regarding material properties, steel yield limits up to 820 MPa and concrete strengths up to 115MPa have been effectively used.

An ANN model, even though time consuming to successfully train, requiring a certain level of expertise in its development, once developed it can be quite valuable in its predictions since it is directly correlated to experimental results. In this context its reliability is always controlled by the range of values of the input variables, available in the experimental database used for its training. Therefore, it is always useful to continually enrich the experimental database with new specimens, so that the reliability of the developed model is furtherly extended and improved.

Nomenclature

ANN(s)	Artificial Neural Network(s)
A_c	Area of Concrete Core Section
A_s	Area of Steel Tube Section
A_{sc}	Area of Composite Section
B	Width of Tubes Section
BPNN	Back Propagation Neural Network
CFST	Concrete Filled Steel Tube
Co	Competitive transfer function
E_c	Concrete Modulus of Elasticity
E_s	Steel Modulus of Elasticity
f'_c	Concrete Compressive Strength
f_y	Steel Yield Limit
f_u	Steel Ultimate Strength
GP	Genetic Programming
GUI	Graphical User Interface
H	Height of Tubes Section
HTS	Hyperbolic Tangent Sigmoid transfer function
I_s	Moment of Inertia of Steel Tube Section
I_c	Moment of Inertia of Concete Core Section
L	Length of Column
L_e	Effective Length of Column
Li	Linear transfer function
LS	Log-Sigmoid transfer function
MAPE	Mean Absolute Percentage Error
MSE	Mean Square Error
N	Axial Load Capacity
N_b	Buckling Capacity of Column
N_{cr}	Elastic Critical Bucking Load
N_{pl}	Squash Load
NRB	Normalized Radial Basis transfer function
PLi	Positive Linear transfer function
R	Pearson correlation coefficient
RB	Radial Basis transfer function
SM	Soft Max transfer function
SSE	Sum Square Error
SP	Superplasticizer
SSL	Symmetric Saturating Linear transfer function
t	Wall Thickness of Steel Tubes
TB	Triangular Basis transfer function
ξ	Confinement Factor
ρ	Concrete Density
$N_u^{predicted}$	Prediction of axial load of CFST columns
[Iw]	Weight matrix of the hidden layer
[bi]	Bias matrix of the hidden layer
[LW]	Weight matrix of the output layer
[bo]	Bias matrix of the output layer
B_{min}, B_{max}	Min and max values of width of tubes sections
H_{min}, H_{max}	Min and max values of height of tubes sections
t_{min}, t_{max}	Min and max values of thickness of tubes sections
L_{emin}, L_{emax}	Min and max values of effective length of column
f_{ymin}, f_{ymax}	Min and max values of steel yield limit
f'_{cmin}, f'_{cmax}	Min and max values of concrete strength

References

ACI 318 (2014), *Building Code Requirements for Structural Concrete and Commentary*, American Concrete Institute, U.S.A.

Ahmadi, M., Naderpour, H. and Kheyroddin, A. (2017). "ANN model for predicting the compressive strength of circular steel-confined concrete." *International Journal of Civil Engineering,* **15**, 213-221.

AIJ (1997), *A.I. of Recommendations for Design and Construction of Concrete Filled Steel Tubular Structures*, Architectural Institute of Japan, Tokyo, Japan

Akbar, H., Suryana, N. and Sahib, S. (2011), "Training neural networks using clonal selection algorithm and particle swarm optimization: A comparisons for 3D object recognition", *2011 11th International Conference on Hybrid Intelligent Systems (HIS),* 692-697.

Al-Khaleefi, A.M., Terro, M.J., Alex, A.P. and Wang, Y. (2002), "Prediction of fire resistance of concrete filled tubular steel columns using neural networks", *Fire Safety J.,* **37**, 339. https://doi.org/10.1016/S0379-7112(01)00065-0.

Alavi, A.H. and Gandomi, A.H. (2012), "Energy-based numerical models for assessment of soil liquefaction", *Geosci. Front.*, **3**(4), 541-555. https://doi.org/10.1016/j.gsf.2011.12.008.

Ali, F., Nadjai, A. and Goodfellow, N. (2016), "Experimental and numerical study on the performance of hollow and concrete-filled elliptical steel columns subjected to severe fire", *Fire Mater.,* **40**, 635-652. https://doi.org/10.1002/fam.2316.

ANSI/AISC 360 (2016), *Specification for Structural Steel Buildings*, American Institute of Steel Construction, Chicago, U.S.A.

Apostolopoulou, M., Armaghani, D.J., Bakolas, A., Douvika, M.G., Moropoulou, A. and Asteris, P.G. (2019), "Compressive strength of natural hydraulic lime mortars using soft computing techniques", *Procedia Struct. Integrity,* **17**, 914-923. https://doi.org/10.1016/j.prostr.2019.08.122.

Apostolopoulou, M., Asteris, P.G., Armaghani, D.J., Douvika, MG., Lourenço, P.B., Cavaleri, L., Bakolas, A. and Moropoulou, A. (2020), "Mapping and holistic design of natural hydraulic lime mortars", *Cement Concrete Res.*, **136**, 106167, https://doi.org/10.1016/j.cemconres.2020.106167.

Aqil, M., Kita, I., Yano, A. and Nishiyama, S. (2007), "A comparative study of artificial neural networks and neuro-fuzzy in continuous modeling of the daily and hourly behaviour of runoff", *J. Hydrology,* **337**, 22-34. https://doi.org/10.1016/j.jhydrol.2007.01.013.

Armaghani, D.J. and Asteris, P.G. (2021), "A comparative study of ANN and ANFIS models for the prediction of cement-based mortar materials compressive strength", *Neural Comput. Appl*., **33**(9), 4501-4532. http://dx.doi.org/10.1007/s00521-020-05244-4

Armaghani, D.J., Hajihassani, M., Sohaei, H., Mohamad, E.T., Marto, A., Motaghedi, H. and Moghaddam, M.R. (2015), "Neuro-fuzzy technique to predict air-overpressure induced by blasting", *Arab. J. Geosci.,* **8**(12), 10937-10950. https://doi.org/10.1007/s12517-015-1984-3.

Armaghani, D.J., Mamou, A., Maraveas, C., Roussis, P.C., Siorikis, V.G., Skentou, A.D. and Asteris, P.G. (2021), "Predicting the unconfined compressive strength of granite using only two non-destructive test indexes", *Geomech. Eng.*, **25**(4).

Armaghani, D.J., Momeni, E. and Asteris, P.G. (2020), "Application of group method of data handling technique in assessing deformation of rock mass", *Metaheuristic Comput. Appl.*, **1**(1), 1-18. http://dx.doi.org/10.12989/mca.2020.1.1.001.

AS5100 (2004), *Australian Standard - Bridge Design, Part 6: Steel and Composite Construction*, Standards Australia International, Sydney, Australia

Aslani, F., Uy, B., Tao, Z. and Mashiri, F., (2015), "Behaviour and design of composite columns incorporating compact high-strength steel plates", *J. Construct. Steel Res.*, **107**, 94-110, https://doi.org/10.1016/j.jcsr.2015.01.005.

Asteris, P.G and Mokos, V.G. (2020), "Concrete compressive strength using artificial neural networks", *Neural Comput. Appl.*, **32**, 1807-11826. https://doi.org/10.1007/s00521-019-04663-2.

Asteris, P.G., Apostolopoulou, M., Skentou, A.D. and Moropoulou, A. (2019), "Application of artificial neural networks for the prediction of the compressive strength of cement-based mortars", *Comput. Concrete,* **24**, 329-345. 10.12989/cac.2019.24.4.329.

Asteris, P.G., Lemonis, M.E., Le, T.T. and Tsavdaridis, K.D. (2021c), "Evaluation of the ultimate eccentric load of rectangular CFSTs using advanced neural network modeling", Eng. Struct., **248**, 113297, https://doi.org/10.1016/j.engstruct.2021.113297.

Asteris, P.G., Lemonis, M.E., Nguyen, T.A., Le, H.V. and Pham, B.T. (2021a). "Soft computing-based estimation of ultimate axial load of rectangular concrete-filled steel tubes", *Steel Compos. Struct.*, **39**(4), 471-491. https://doi.org/10.12989/scs.2021.39.4.471.

Asteris, P.G., Lourenço, P.B., Hajihassani, M., Adami, C.E.N., Lemonis, M.E., Skentou, A.D., Marques, R., Nguyen, H., Rodrigues, H. and Varum, H. (2021d), "Soft computing based models for the prediction of masonry compressive strength", Eng. Struct., **248**, 113276, https://doi.org/10.1016/j.engstruct.2021.113276.

Asteris, P.G., Skentou, A.D., Bardhan, A., Samui, P., Pilakoutas, K. (2021b), "Predicting concrete compressive strength using hybrid ensembling of surrogate machine learning models", *Cement Concrete Res.*, 2021, **145**, 106449, https://doi.org/10.1016/j.cemconres.2021.106449.

Baig, M.N., Fan, J. and Nie, J. (2006), "Strength of concrete filled steel tubular columns", *Tsinghua Science Technol.,* **11**, 657-666.

Battiti, R. (1992), "First- and second-order methods for learning: Between steepest descent and newton's method." *Neural Comput.,* **4**, 141-166. https://doi.org/10.1162/neco.1992.4.2.141.

Behnam, A. and Esfahani, M.R. (2018). "Prediction of biaxial bending behavior of steel-concrete composite beam-columns by artificial neural network", *Iran Univ. Sci. Technol.,* **8**, 381-399.

Bradford, M.A., Loh, H.Y. and Uy, B. (2002), "Slenderness limits for filled circular steel tubes", *J. Construct. Steel Res.,* **58**, 243-252. https://doi.org/10.1016/S0143-974X(01)00043-8.

Brownlee, J. (2016), *Master Machine Learning Algorithms: Discover How They Work and Implement Them From Scratch*, https://books. google. ca/books.

Caprili, S. and Salvatore, W. (2015), "Cyclic behaviour of uncorroded and corroded steel reinforcing bars", *Construct. Build. Mater.,* **76**, 168-186. https://doi.org/10.1016/j.conbuildmat.2014.11.025.

Cederwall, K., Engstrom, B. and Grauers, M., (1990), "High-Strength Concrete Used in Composite Columns", *ACI Symposium Publication*, **121**, 195-214.

Chang, X., Wei, Y.Y. and Yun, Y.C. (2012), "Analysis of steel-reinforced concrete-filled-steel tubular (SRCFST) columns under cyclic loading", *Construct. Build. Mater.* **28**, 88-95. https://doi.org/10.1016/j.conbuildmat.2011.08.033.

Chen, J. and Jin, W., (2010), "Experimental investigation of thin-walled complex section concrete-filled steel stub columns", *Thin-Wall. truct.* **48(**9), 718-724, https://doi.org/10.1016/j.tws.2010.05.001.

Chen, S., Zhang, R., Jia, LJ., Wang, JY. and Gu, P., (2018), "Structural behavior of UHPC filled steel tube columns under axial loading", *Thin-Wall. Struct.*, **130**, 550-563, https://doi.org/10.1016/j.tws.2018.06.016.

Choi, K.K. and Xiao, Y. (2009). "Analytical studies of concrete-filled circular steel tubes under axial compression", *J. Struct. Eng.,* **136**, 565-573. https://doi.org/10.1061/(ASCE)ST.1943-541X.0000156.

Chung, J., Matsui, C. and Tsuda, K., (2001), "Simplified design formula of slender concrete filled steel tubular beam-columns", *Struct. Eng. Mech.*, **12**(1), 71-84, https://doi.org/10.12989/sem.2001.12.1.071.

Dai, X. and Lam, D. (2010), "Numerical modelling of the axial compressive behaviour of short concrete-filled elliptical steel columns", *J. Construct. Steel Res.,* **66**, 931-942. https://doi.org/10.1016/j.jcsr.2010.02.003.

DBJ13-51-2010 (2010), *Technical Specification for Concrete-filled Steel Tubular Structures*, The Construction Department of Fujian Province, Fuzhou, China

Du, K.L. and Swamy, M.N. (2013), *Neural Networks and Statistical Learning,* Springer Science & Business Media.

Du, Y., Chen, Z. and Xiong, M.X., (2016), "Experimental behavior and design method of rectangular concrete-filled tubular columns using Q460 high-strength steel", *Construct. Build. Mater.*, **125**, 856-872, https://doi.org/10.1016/j.conbuildmat.2016.08.057.

Du, Y., Chen, Z. and Yu, Y., (2016), "Behavior of rectangular concrete-filled high-strength steel tubular columns with different aspect ratio", *Thin-Wall. Struct.*, **109**, 304-318, https://doi.org/10.1016/j.tws.2016.10.005.

Du, Y., Chen, Z., Zhang, C. and Cao, X. (2017), "Research on axial bearing capacity of rectangular concrete-filled steel tubular columns based on artificial neural networks", *Front. Comput. Sci.,* **11**, 863-873. https://doi.org/10.1007/s11704-016-5113-6.

Dundu, M., (2016), "Column buckling tests of hot-rolled concrete filled square hollow sections of mild to high strength steel", *Eng. Struct.*, **127**, 73-85, https://doi.org/10.1016/j.engstruct.2016.08.039.

Duong, H.T., Phan, H.C., Le, T.T. and Bui, N.D. (2020), "Optimization design of rectangular concrete-filled steel tube short columns with Balancing Composite Motion Optimization and data-driven model", *Struct.*, **28**, 757-765. https://doi.org/10.1016/j.istruc.2020.09.013.

EN1994 (2004), *Eurocode 4 - Design of composit e steel and concrete structures - Part 1-1: General Rules and Rules for Buildings*, CEN, Brussels, Belgium.

Fam, A., Qie, F.S. and Rizkalla, S. (2004), "Concrete-filled steel tubes subjected to axial compression and lateral cyclic loads", *J. Struct. Eng.,* **130**, 631-640. https://doi.org/10.1061/(ASCE)0733-9445(2004)130:4(631).

Furlong, R.W., (1967), "Strength of steel-encased concrete beam columns", *J. Struct. Div.*, **93**(5), 113-124. https://doi.org/10.1061/JSDEAG.0001761.

Ghannam, S., Jawad, Y.A. and Hunaiti, Y. (2004), "Failure of lightweight aggregate concrete-filled steel tubular columns", *Steel Compos. Struct.*, **4**(1), 1-8. https://doi.org/10.12989/scs.2004.4.1.001.

Giakoumelis, G. and Lam, D. (2004), "Axial capacity of circular concrete-filled tube columns", *J. Construct. Steel Res.,* **60**, 1049-1068. https://doi.org/10.1016/ j.jcsr.2003.10.001.

Goel, T. and Tiwary, A. (2018), "Finite element modeling of Circular Concrete Filled Steel Tube (CFST)", *Indian J. Sci. Technol.,* **11**, 1-9. https://doi.org/10.17485/ijst/2018/v11i34/130853.

Grauers, M. (1993), *Composite Columns of Hollow Steel Sections Filled with High Strength Concrete*, Ph.D. Dissertation,

Chalmers University of Technology, Göteborg.
Guo, L. (2006), *Theoretical and Experimental Research on the Behavior of Concrete-Filled Rectangular Hollow Section Steel Tubes*, PhD Dissertation, Harbin Institute of Technology, Harbin.
Guo, L., Zhang, S., Wang, Y. and Liu, J., (2005), "Analytical and experimental research on axially loaded slender HSC filled RHS steel tubular columns", *Indus. Construct.*, **35**(3),75-79.
Guo, L.H., Zhang, S.M. and Kim, W.J., (2006), "Elastic and elastic-plastic buckling behavior of SHS steel tube filled with concrete", *Harbin Gongye Daxue Xuebao/Journal of Harbin Institute of Technology*, **38**(8), 1350-1354.
Gupta, R., Gijzen van, M.B. and Vuik, C.K. (2013), "Efficient Two-Level Preconditioned Conjugate Gradient Method on the GPU", In *High Performance Computing for Computational Science - VECPAR 2012*, 36-49. Springer, Berlin. https://doi.org/10.1007/978-3-642-38718-0_7.
Han, L.H, Yao, G.H. and Zhao, X.L. (2005), "Tests and calculations for hollow structural steel (HSS) stub columns filled with self-consolidating concrete (SCC)", *J. Construct. Steel Res.*, **61**(9), 1241-1269. https://doi.org/10.1016/j.jcsr.2005.01.004.
Han, L.H. (2002), "Tests on stub columns of concrete-filled RHS sections", *J. Construct. Steel Res.*, **58**(3), 353-372. https://doi.org/10.1016/S0143-974X(01)00059-1.
Han, L.H. and Yang, Y.F. (2001), "Influence of concrete compaction on the behavior of concrete filled steel tubes with rectangular sections", *Adv. Struct. Eng.,* **4**, 93-100. https://doi.org/10.1260/1369433011502381.
Han, L.H. and Yang, Y.F., (2003), "Analysis of thin-walled steel RHS columns filled with concrete under long-term sustained loads", *Thin-Wall. Struct.*, **41**(9), 849-870. https://doi.org/10.1016/S0263-8231(03)00029-6.
Han, L.H. and Yao, G.H. (2003), "Influence of concrete compaction on the strength of concrete-filled steel RHS columns", *J. Construct. Steel Res.*, **59**(6), 751-767. https://doi.org/10.1016/S0143-974X(02)00076-7.
Han, L.H. and Yao, G.H. (2004), "Experimental behavior of thin-walled hollow structural steel (HSS) columns filled with self-consolidating concrete (SCC)", *Thin-Wall. Struct.*, **42**(9), 1357-1377, https://doi.org/10.1016/j.tws.2004.03.016.
Han, L.H. and Yao, G.H., (2003), "Behavior of concrete-filled hollow structural steel (HSS) columns with pre-load on the steel tubes", *J. Construct. Steel Res.*, **59**(12), 1455-1475, https://doi.org/10.1016/S0143-974X(03)00102-0.
Han, L.H., Hou, C. and Wang, Q.L. (2012), "Square concrete filled steel tubular (CFST) members under loading and chloride corrosion: experiments", *J. Construct. Steel Res.,* **71**, 11-25. https://doi.org/10.1016/j.jcsr.2011.11.012.
Han, L.H., Huo, J.S. and Wang, Y.C. (2005), "Compressive and flexural behaviour of concrete filled steel tubes after exposure to standard fire", *J. Construct. Steel Res.,* **61**, 882-901. https://doi.org/10.1016/j.jcsr.2004.12.005.
Han, L.H., Li, W. and Bjorhovde, R. (2014), "Developments and advanced applications of concrete-filled steel tubular (CFST) structures: Members", *J. Construct. Steel Res.,* **100**, 211-228. https://doi.org/10.1016/j.jcsr.2014.04.016.
Ho, N.X. and Le, T.T. (2021), "Effects of variability in experimental database on machine-learning-based prediction of ultimate load of circular concrete-filled steel tubes", *Measurement*, **176**, 109198. https://doi.org/10.1016/j.measurement.2021.109198.
Hossain, K.M.A. and Chu, K, (2019), "Confinement of six different concretes in CFST columns having different shapes and slenderness", *Int. J. Adv. Struct. Eng.,* **11**, 255-270. https://doi.org/10.1007/s40091-019-0228-2.
Huang, L., Asteris, P.G., Koopialipoor, M., Armaghani, D.J. and Tahir, M.M. (2019), "Invasive weed optimization technique-based ANN to the rediction of rock tensile strength", *Appl. Sci.* **9**, 5372. https://doi.org/10.3390/app9245372.
Huang, Z., Uy, B., Li, D. and Wang, J., (2020), "Behavior and design of ultra-high-strength CFST members subjected to compression and bending", *J. Construct. Steel Res.*, **175**. https://doi.org/10.1016/j.jcsr.2020.106351.
Ibañez, C., Hernández-Figueirido, D. and Piquer, A. (2018), "Shape effect on axially loaded high strength CFST stub columns", *J. Construct. Steel Res.*, **147**, 247-256, https://doi.org/10.1016/j.jcsr.2018.04.005.
Ibanez, C., Hernández-Figueirido, D. and Piquer, A. (2021), "Effect of steel tube thickness on the behaviour of CFST columns: Experimental tests and design assessment", *Eng. Struct.*, **230**, 111687. https://doi.org/10.1016/j.engstruct.2020.111687.
Ibañez, C., Hernández-Figueirido, D. and Piquer, A. (2021), "Effect of steel tube thickness on the behaviour of CFST columns: Experimental tests and design assessment", *Eng. Struct.*, **230**. https://doi.org/10.1016/j.engstruct.2020.111687.
Inai, E. and Sakino, K. (1996), "Simulation of flexural behavior of square concrete filled steel tubular columns", *Proceedings of the Third Joint Technical Coordinating Committee Meeting, U.S.-Japan Cooperative Research Program, Phase 5: Composite and Hybrid Structures, Hong Kong, National Science Foundation*, Arlington, Virginia.
Islam, M.M., Ali, R.B., Begum, M. and Rahman M.S. (2021), "Experimental study of square concrete-filled welded cold-formed steel columns under concentric Loading", *Arab. J. Sci. Eng.* **46**, 4225-4237. https://doi.org/10.1007/s13369-020-04797-9.
Jegadesh, J. and Jayalekshmi, S. (2015), "A review on artificial neural network concepts in structural engineering applications", *Int. J. Appl. Civil Environ. Eng.,* **1**, 6-11.
Jegadesh, S. and Jayalekshmi, S. (2015b), "Application of artificial neural network for calculation of axial capacity of circular concrete filled steel Tubular Columns", *Int. J. Earth Sci. Eng.,* **8**, 35-42.
Kayacan, E. and Khanesar, M.A. (2015), *Fuzzy Neural Networks for Real Time Control Applications: Concepts, Modeling and Algorithms for Fast Learning.* 1. Butterworth-Heinemann.
Kechagias, J., Tsiolikas, A., Asteris, P. and Vaxevanidis, N. (2018), "Optimizing ANN performance using DOE: Application on turning of a titanium alloy", MATEC Web of Conferences, 178, 01017.
Khan, M., Uy, B., Tao, Z. and Mashiri, F. (2017), "Behaviour and design of short high-strength steel welded box and concrete-filled tube (CFT) sections", *Eng. Struct.*, **147**, 458-472. https://doi.org/10.1016/j.engstruct.2017.06.016.
Khan, M., Uy, B., Tao, Z. and Mashiri, F., (2017), "Concentrically loaded slender square hollow and composite columns incorporating high strength properties", *Eng. Struct.*, **131**, 69-89. https://doi.org/10.1016/j.engstruct.2016.10.015.
Khanouki, M.M.A., Ramli Sulong, N.H., Shariati, M. and Tahir, M.M. (2016), "Investigation of through beam connection to concrete filled circular steel tube (CFCST) column", *J. Construct. Steel Res.,* **121**, 144-162. https://doi.org/10.1016/j.jcsr.2016.01.002.
Knowles, R.B. and Park, R. (1969), "Strength of concrete filled steel tubular columns", *J. Struct. Div.*, **95**(12), 2565-2588. https://doi.org/10.1061/JSDEAG.0002425.
Krishan, A.L., Chernyshova, E.P. and Sabirov, R.R. (2016), "Calculating the strength of concrete filled steel tube columns of solid and ring cross-section", *Procedia Engineering,* **150**, 1878-1884. https://doi.org/10.1016/ j.proeng.2016.07.186.
Lam, D. and Williams, C.A. (2004), "Experimental study on concrete filled square hollow sections", *Steel Compos. Struct.*,

4(2), 95-112, https://doi.org/10.12989/ scs.2004.4.2.095.

Liew, JR., Xiong, M. and Xiong, D. (2016), "Design of concrete filled tubular beam-columns with high strength steel and concrete", *Structures*, **8**, 213-226. https://doi.org/10.1016/ j.istruc.2016.05.005.

Lin, C.Y. (1988), "Axial capacity of concrete infilled cold-formed steel columns", *Ninth International Specialty Conference on Cold-Formed Steel Structures*, St. Louis, Missouri, U.S.A.

Liu, D. (2005), "Tests on high-strength rectangular concrete-filled steel hollow section stub columns", *J. Construct. Steel Res.*, **61**(7), 902-911. https://doi.org/10.1016/ j.jcsr.2005.01.001.

Liu, D. and Gho, W.M. (2005), "Axial load behavior of high-strength rectangular concrete-filled steel tubular stub columns", *Thin-Wall. Struct.*, **43**(8), 1131-1142. https://doi.org/10.1016/j.tws.2005.03.007.

Liu, D., Gho, W.M. and Yuan, J. (2003), "Ultimate capacity of high-strength rectangular concrete-filled steel hollow section stub columns", *J. Construct. Steel Res.*, **59**(12), 1499-1515. https://doi.org/10.1016/S0143-974X(03)00106-8.

Liu, S., Ding, X., Li, X., Liu, Y. and Zhao, S. (2019), "Behavior of rectangular-sectional steel tubular columns filled with high-strength steel fiber reinforced concrete under axial compression", *Materials,* **12**, 2716. https://doi.org/10.3390/ma12172716.

Lourakis, M.I.A. (2005), "A brief description of the Levenberg-Marquardt algorithm implemented by levmar", Hellas (FORTH), Institute of Computer Science Foundation for Research and Technology, http://www.ics.forth.gr/~lourakis/levmar/levmar.

Lu, D., Gong, Y., Ding, F., Wang, L., Deng, C., Yuan, T., Chen, L. and Ren, E. (2021), "Experimental study of square CFST stub columns with a low steel ratio under axial loading", *Front. Materials*, **8**(52), https://doi.org/10.3389/fmats.2021.629819.

Lu, Y.Q. and Kennedy, D.J.L. (1994), "The flexural behavior of concrete-filled hollow structural sections", *Can. J. Civ. Eng.*, **21**(1), 111-130. https://doi.org/10.1139/l94-011.

Lu, X., Yu, Y. and Chen, Y., (1999), "Studies on the behavior of concrete-filled rectangular tubular short column: 1 Experiment", *Build. Struct.*, **29**(10), 41-43.

Lue, D.M., Liu, J.L. and Yen, T. (2007), "Experimental study on rectangular CFT columns with high-strength concrete", *J. Construct. Steel Res.*, **63**(1), 37-44. https://doi.org/10.1016/j.jcsr.2006.03.007.

Luo, L. (1986), Experimental Research on Long Filled Concrete Square Steel Tube Columns Under Axial Compressive Load, Masters Thesis, Zhengzhou University of Technology. Zhengzhou.

Ly, H.B., Pham, B.T., Le, L.M., Le, T.T., Le, V.M. and Asteris, P.G. (2021), "Estimation of axial load-carrying capacity of concrete-filled steel tubes using surrogate models", *Neural Comput. Appl.*, **33**(8), 3437-3458. https://doi.org/10.1007/s00521-020-05214-w.

Marquardt, D. (1963), "An algorithm for least-squares estimation of nonlinear parameters", *J. Soc. Ind. Appl. Mathem.,* **11**, 431-441. https://doi.org/10.1137/0111030.

Matsui, C. and Tsuda, K. (1996), "Strength and behavior of slender concrete filled steel tubular columns", *Proceedings of The Second International Symposium on Civil Infrastructure Systems.* Hong Kong, China.

Matsui, C., Tsuda, K. and Ishibashi, Y. (1995), "Slender concrete filled steel tubular columns under combined compression and bending", *Structural Steel, PSSC95, 4th Pacific Structural Steel Conference*, 3, Singapore.

Møller, M.F. (1993), "A scaled conjugate gradient algorithm for fast supervised learning", *Neural Networks,* **6**, 525-533. https://doi.org/10.1016/S0893-6080(05)80056-5.

Momeni, E., Armaghani, D.J., Hajihassani, M. and Amin, M.F.M. (2015), "Prediction of uniaxial compressive strength of rock samples using hybrid particle swarm optimization-based artificial neural networks", *Measurement*, **60**, 50-63. https://doi.org/10.1016/j.measurement.2014.09.075.

Mursi, M. and Uy, B. (2004), "Strength of slender concrete filled high strength steel box columns", *J. Construct. Steel Res.*, **60**(12), 1825-1848. https://doi.org/10.1016/j.jcsr.2004.05.002.

Nakahara, H. and Sakino, K. (1998), "Axial compressive and uniform bending tests of high strength concrete filled square steel tubular columns", *Proceedings of the Fifth Pacific Structural Steel Conference*, Seoul, Korea.

Nguyen, T.T., Thai, H.T., Ngo, T., Uy, B. and Li, D. (2021), "Behavior and design of high strength CFST columns with slender sections", *J. Construct. Steel Res.*, **182**, https://doi.org/10.1016/j.jcsr.2021.106645.

Powell, M.J.D. (1977), "Restart procedures for the conjugate gradient method", *Mathematical Programming,* **12**, 241-254. https://doi.org/10.1007/BF01593790.

Psyllaki, P., Stamatiou, K., Iliadis, I., Mourlas, A., Asteris, P. and Vaxevanidis, N. (2018), "Surface treatment of tool steels against galling failure", *MATEC Web of Conferences*, 188, 04024.

Raghuwanshi, N.S., Singh, R. and Reddy, L.S. (2006), "Runoff and Sediment Yield Modeling Using Artificial Neural Networks: Upper Siwane River, India", *J. Hydrol. Eng.,* **11**, 71-79. https://doi.org/10.1061/(ASCE)1084-0699(2006)11:1(71).

Ren, Q., Li, M., Zhang, M., Shen, Y. and Si, W. (2019), "Prediction of Ultimate Axial Capacity of Square Concrete-Filled Steel Tubular Short Columns Using a Hybrid Intelligent Algorithm", *Appl. Sci.,* **9**, 2802. https://doi.org/10.3390/app9142802.

Rumelhart, D.E., Hinton, G.E. and Williams, R.J. (1986), "Learning representations by back-propagating errors", *Nature,* **323**, 533-536. https://doi.org/10.1038/323533a0.

Sakino, K. Nakahara, H., Morino, S. and Nishiyama, I., (2004), "Behavior of centrally loaded concrete-filled steel-tube short columns", *J. Struct. Eng.*, **130**(2), 180-188. https://doi.org/10.1061/(ASCE)0733-9445(2004)130:2(180).

Sarir, P., Chen, J., Asteris, P.G., Armaghani, D.J. and Tahir, M.M. (2019a), "Developing GEP tree-based, neuro-swarm, and whale optimization models for evaluation of bearing capacity of concrete-filled steel tube columns", *Eng. Comput.,* https://doi.org/10.1007/s00366-019-00808-y.

Sarir, P., Shen, S.L., Wang, Z.F., Chen, J., Horpibulsuk, S. and Pham, B.T. (2019b), "Optimum model for bearing capacity of concrete-steel columns with AI technology via incorporating the algorithms of IWO and ABC", *Eng. Comput.,* **37**, 797-807. https://doi.org/10.1007/s00366-019-00855-5.

Schneider, S.P. (1998), "Axially loaded concrete-filled steel tubes", *J. Struct. Eng.*, **124**(10), 1125-1138. https://doi.org/10.1061/(ASCE)0733-9445(1998)124:10(1125).

Shakir-Khalil, H. and Mouli, M. (1990), "Further tests on concrete-filled rectangular hollow-section columns", *Struct. Engineer*, **68**(20), 405-413.

Song, T.Y., Tao, Z., Han, L.H. and Uy, B. (2017), "Bond behavior of concrete-filled steel tubes at elevated temperatures", *J. Struct. Eng.,* **143**, 04017147. https://doi.org/10.1061/(ASCE)ST.1943-541X.0001890.

Tao, Z., Han, L.H. and Wang, D.Y. (2008), "Strength and ductility of stiffened thin-walled hollow steel structural stub columns filled with concrete", *Thin-Wall. Struct.*, **46**(10), 1113-1128, https://doi.org/10.1016/j.tws.2008.01.007.

Tao, Z., Song, T.Y., Uy, B. and Han, L.H. (2016), "Bond behavior in concrete-filled steel tubes", *J. Construct. Steel Res.,* **120**, 81-93. https://doi.org/10.1016/j.jcsr.2015.12.030.

Tao, Z., Uy, B., Han, L.H. and Wang, Z.B. (2009), "Analysis and design of concrete-filled stiffened thin-walled steel tubular columns under axial compression", *Thin-Wall. Struct.*, **47**(12), 1544-1556. https://doi.org/10.1016/j.tws.2009.05.006.

Taormina, R., Chau, K. and Sethi, R. (2012), "Artificial neural network simulation of hourly groundwater levels in a coastal aquifer system of the Venice lagoon", *Eng. Appl. Artif. Intel.,* **25**, 1670-1676. https://doi.org/10.1016/j.engappai.2012.02.009.
Tomii, M. and Sakino, K. (1979), "Experimental studies on the ultimate moment of concrete filled square steel tubular beam-columns", *Transactions Architect. Institute Japan*, **275**, 55-65. https://doi.org/10.3130/aijsaxx.275.0_55.
Uy, B. (1998), "Local and post-local buckling of concrete filled steel welded box columns", *J. Construct. Steel Res.*, **47**(1-2), 47-72. https://doi.org/10.1016/S0143-974X(98)80102-8.
Uy, B. (2000), "Strength of concrete filled steel box columns incorporating local buckling", *J. Struct. Eng.*, **126**(3), 341-352, https://doi.org/10.1061/(ASCE)0733-9445(2000)126:3(341).
Vos de, N.J. and Rientjes, T.H.M. (2008), "Multiobjective training of artificial neural networks for rainfall-runoff modeling", *Water Resource. Res.,* **44**. https://doi.org/10.1029/2007WR006734.
Vrcelj, Z. and Uy, B. (2002), "Behavior and design of steel square hollow sections filled with high strength concrete", *Aust. J. Struct. Eng.*, **3**(3), 153-170. https://doi.org/10.1080/13287982.2002.11464902.
Wang, Z.B., Tao, Z., Han, L.H., Uy, B., Lam, D. and Kang, W.H. (2017), "Strength, stiffness and ductility of concrete-filled steel columns under axial compression", *Eng. Struct.*, **135**, 209-221. https://doi.org/10.1016/j.engstruct.2016.12.049.
Wei, Z. and Han, L. (2000), "Research on the bearing capacity of early-strength concrete filled square steel tube", *Proceedings 6th ASCCS Conference; Composite and Hybrid Structures*, Los Angeles.
Xiao, Y.F. (2012), "Approach of concrete-filled steel tube ultrasonic method based on ANN", *Appl. Mech. Mater.,* **105**, 1611-1615. https://doi.org/10.4028/www.scientific.net/AMM.105-107.1611.
Xiong, M.X., Xiong, DX. and Liew, J.R. (2017), "Axial performance of short concrete filled steel tubes with high-and ultra-high-strength materials", *Eng. Struct.*, **136**, 494-510. https://doi.org/10.1016/j.engstruct.2017.01.037.
Yamamoto, T., Kawaguchi, J. and Morino, S. (2000), "Experimental study of scale effects on the compressive behavior of short concrete-filled steel tube columns", *Compos. Construct. Steel Concrete IV Conference*, https://doi.org/10.1061/40616(281)76.
Yan, J.B., Dong, X. and Wang, T. (2020), "Axial compressive behaviours of square CFST stub columns at low temperatures", *J. Construct. Steel Res.*, **164**, https://doi.org/10.1016/j.jcsr.2019.105812.
Ye, Z. (2001), *Compressive Behavior of High-Strength Concrete-Filled Square and Rectangular Steel Tubes*, Master Thesis, Harbin Institute of Technology, Harbin.
Young, B. (2008), "Experimental and numerical investigation of high strength stainless steel structures", *J. Construct. Steel Res.,* **64**, 1225-1230. https://doi.org/10.1016/j.jcsr.2008.05.004.
Yu, M., Zha, X., Ye, J. and Li, Y. (2013), "A unified formulation for circle and polygon concrete-filled steel tube columns under axial compression", *Eng. Struct.,* **49**, 1-10. https://doi.org/10.1016/j.engstruct.2012.10.018.
Yu, Q., Tao, Z. and Wu, Y.X. (2008), "Experimental behaviour of high performance concrete-filled steel tubular columns", *Thin-Wall. Struct.*, **46**(4), 362-370. https://doi.org/10.1016/j.tws.2007.10.001.
Yu, Z., Ding, F. and Cai, C.S. (2007), "Experimental behavior of circular concrete-filled steel tube stub columns", *J. Construct. Steel Res.,* **63**, 165-174. https://doi.org/10.1016/j.jcsr.2006.03.009.
Zeng, J., Asteris, P.G., Mamou, A.P., Mohammed, A.S., Golias, E.A., Armaghani, D.J., Faizi, K.; Hasanipanah, M. (2021), "The effectiveness of ensemble-neural network techniques to predict peak uplift resistance of buried pipes in reinforced sand", *Appl. Sci.*, **2021**(11), 908. https://doi.org/10.3390/app11030908.
Zhang, H., Nguyen, H., Bui, X.N., Pradhan, B., Asteris, P.G., Costache, R. and Aryal, J. (2021), "A generalized artificial intelligence model for estimating the friction angle of clays in evaluating slope stability using a deep neural network and Harris Hawks optimization algorithm", *Eng. Comput.*, 1-14. https://doi.org/10.1007/s00366-020-01272-9.
Zhang, S. and Zhou, M. (2000), "Stress-strain behavior of concrete-filled square steel tubes", *Proceedings 6th ASCCS Conference; Composite and Hybrid Structures*, Los Angeles.
Zhang, Z. (1984), *Experimental Research on Short Filled Concrete Square Steel Tube Columns Under Axial Compressive Load*, Master thesis, Harbin University of Technology, Harbin.
Zhao, O., Rossi, B., Gardner, L. and Young, B. (2015), "Behaviour of structural stainless steel cross-sections under combined loading–Part I: Experimental study", *Eng. Struct.,* **89**, 236-246. https://doi.org/10.1016/j.engstruct.2014.11.014.
Zhou, X., Zhou, Z. and Gan, D. (2020), "Analysis and design of axially loaded square CFST columns with diagonal ribs", *J. Construct. Steel Res.*, **167**, https://doi.org/10.1016/j.jcsr.2019.105848.
Zhu, A., Zhang, X., Zhu, H., Zhu, J. and Lu, Y., (2017), "Experimental study of concrete filled cold-formed steel tubular stub columns", *J. Construct. Steel Res.*, **134**, 17-27. https://doi.org/10.1016/j.jcsr.2017.03.003.
Zhu, J.Y. and Chan, T.M. (2018), "Experimental investigation on octagonal concrete filled steel stub columns under uniaxial compression", *J. Construct. Steel Res.*, **147**, 457-467, https://doi.org/10.1016/ j.jcsr.2018.04.030.

BU

Appendix

In Table 9 the expressions provided by the design codes that were utilized in this work are presented, omitting safety factors.

Table 9 Expressions in design codes for the CFST axial compressive strength

Code	Formulas for axial compressive strength
EN1994 (2004)	$N^{EC4} = \chi N_{pl}$, Where: – χ depending on $\bar{\lambda}$ and imperfections, $\chi \le 1$, – $N_{pl} = f_y A_s + f_c' A_c$ – $\bar{\lambda} = \sqrt{N_{pl}/N_{cr}}$ – $N_{cr} = \pi^2 (EI)_{eff}/{L_e}^2$ – $(EI)_{eff} = E_s I_s + 0.6 E_c I_c$
AISC 360 (2016)	$N^{AISC360} = \begin{cases} N_{no}\left(0.658^{\left(\frac{N_{no}}{N_{cr}}\right)}\right) & , \frac{N_{no}}{N_{cr}} \le 2.25 \\ 0.877 N_{cr} & , \frac{N_{no}}{N_{cr}} > 2.25 \end{cases}$ Where: – $N_{no} =$ $\begin{cases} N_{pl} & , \lambda < \lambda_p \\ N_{pl} - (N_{pl} - N_y)\frac{(\lambda-\lambda_p)^2}{(\lambda_r-\lambda_p)^2} & , \lambda_p \le \lambda < \lambda_r \\ 9E_s A_s/(\lambda^2 + 0.7 f_c' A_c) & , \lambda \ge \lambda_r \end{cases}$ – $N_{pl} = f_y A_s + 0.85 f_c' A_c$ – $N_y = f_y A_s + 0.7 f_c' A_c$ – $\lambda = (H - 2t)/t$ – $\lambda_p = 2.26\sqrt{E_s/f_y}$, $\lambda_r = 3.00\sqrt{E_s/f_y}$ – $(EI)_{eff} = E_s I_s + C_3 E_c I_c$ – $C_3 = 0.45 + 3A_c/A_{sc} \le 0.9$
AIJ (1997)	$N^{AIJ} = \begin{cases} A_s f_y + 0.85 A_c f_c' \ (= N_{pl}) & , \lambda \le 4 \\ N_{pl} - \frac{1}{8}(N_{pl} - N_b)(\lambda - 4) & , 4 < \lambda \le 12 \\ N_b^c + N_b^s \ (= N_b) & , \lambda > 12 \end{cases}$ Where: – $\lambda = L_e/B$ – $N_b^c = \begin{cases} \frac{2}{1+\sqrt{\bar{\lambda}_c^4+1}} 0.85 A_c f_c' & , \bar{\lambda}_c \le 1 \\ 0.83 e^{[C_c(1-\bar{\lambda}_c)]} 0.85 A_c f_c' & , \bar{\lambda}_c > 1 \end{cases}$ – $N_b^s =$ $\begin{cases} A_s f_y & , \bar{\lambda}_s < 0.3 \\ [1 - 0.545(\bar{\lambda}_s - 0.3)] A_s f_y & , 0.3 \le \bar{\lambda}_s < 1.3 \\ \pi^2 E_s I_s/(1.3 {L_e}^2) & , \bar{\lambda}_s \ge 1.3 \end{cases}$ – $\bar{\lambda}_c = \lambda_c \sqrt{\varepsilon_u^c}/\pi$ – $\bar{\lambda}_s = (\lambda_s/\pi)\sqrt{f_y/E_s}$ – $\varepsilon_u^c = 0.00093(0.85 f_c')^{0.25}$ – $C_c = 0.568 + 0.00612 f_c'$
AS5100 (2004)	$N^{AS5100} = a_c N_{pl}$, with $a_c \le 1$ Where: – $N_{pl} = f_y A_s + f_c' A_c$ – $N_{cr} = \pi^2 (E_s I_s + E_c I_c)/{L_e}^2$ – $a_c = \xi\left[1 - \sqrt{1 - (90/\xi\lambda)^2}\right]$ – $\lambda = 90\lambda_r + a_a a_b$ – $\lambda_r = \sqrt{N_{pl}/N_{cr}}$ – $\xi = \frac{(\lambda/90)^2 + 1 + \eta}{2(\lambda/90)^2}$ – $a_a = \frac{2100(90\lambda_r - 13.5)}{8100{\lambda_r}^2 - 1377\lambda_r + 2050}$ – $\eta = 0.00326(13.5 - \lambda) \ge 0$